

INTERACTIVE ANALYSIS OF SPACE FRAME RAFT SOIL SYSTEM

J. Noorzai

*Department of Civil Engineering
College of Engineering
University of Shahid Chamran
Ahwaz, Iran*

Abstract This study presents a new approach for physical and material modelling of space frame-raft-soil system. The physical modelling consists of a modified Timoshenko beam bending element with six degrees of freedom per node to model the beams and columns of the superstructure, a modified Mindlin's plate bending element with five degrees of freedom per node to represent the structural slabs and raft, and the coupled finite-infinite elements with three degrees of freedom per node to model the soil media. The constitutive modelling involves the use of the hyperbolic model to account for the soil nonlinearity. The applicability of the proposed physical model is demonstrated by analysing a four storey, five bay by three bay space frame. Moreover, an attempt has been made to compare the linear and nonlinear interactive behavior of the space frame-raft-soil system.

Key Words Physical Modelling, Constitutive Modelling Modified Timoshenko's Beam Bending Element, Seredipity, Hyperbolic Model, Junction Treatment

چکیده در این مقاله روش جدیدی جهت مدل کردن فیزیکی و موادی قابهای فضائی، پی رادیه و خاک ارائه گردیده است. در مدل بندی فیزیکی از تیر اصلاح شده تیموشنکو با ۶ درجه آزادی در هر گره، جهت نشان دادن تیر و ستون، صفحه اصلاح شده میندین با ۵ درجه آزادی در هر گره، برای نشان دادن دال طبقات و پی رادیه و المانهای محدود. نامحدود با سه درجه آزادی در هر گره برای مدل کردن خاک استفاده گردیده است. لازم به توضیح است که در این مقاله مدل هیپربولیک (Duncan-Model) جهت رفتار غیر خطی خاک منظور گردیده است. کاربرد این روش با تحلیل یک قاب فضائی ۴ طبقه (۵ × ۳) نشان داده شده است. سازه فوق الذکر به طریق خطی نیز آنالیز، و نتایج بدست آمده با آنالیز غیر خطی مقایسه گردیده است.

INTRODUCTION

The physical and material modelling of the space frame-raft-soil system has been the concern of the various researchers for a long time. Haddadin [1] proposed the substructure approach for investigating the effect of interaction on the behavior of the space frames, and Hain and Lee [2] proposed the rational analysis of space frame-raft-soil system. The supporting soil was represented by either of the two types of soil models (Winkler and half space models). Comparison of the interactive behavior of a seven storey space frame was made using either of the two soil models. King et al. [3,4,5] suggested the finite

element method for the analysis of rafted multistoreyed space frames. Sankaran and Srinivasaraghavan [6,7] presented a parametric study illustrating the effect of the relative stiffness between superstructure and foundation and that between soil and the foundation on differential settlement of a square raft resting on an elastic homogeneous soil system using the finite element method. The effect of the progressive loading on the interactive behavior of the space frame was studied by Nayak et al. [8] and Brown et. al. [9]

The review of the literature indicates that most of the early investigators represent the supporting soil mass by either the winkler on the half space models

where a linear stress-strain relationship for the soil was assumed. The finite element modelling was based on the truncation approach. Moreover, the effect of stiffness of structural slab on the interactive behavior of the structure-foundation-soil system was ignored.

Thus, keeping the above shortcomings in mind an attempt is made in this study to account for: (a)- an improvement in the physical modelling in terms of physical representation and computational cost (b)-a nonlinear stress-strain relationship of the soil, and (c)-the representation of the structural slab as an integral part of the superstructure.

PHYSICAL MODELLING OF SPACE FRAME-RAFT-SOIL SYSTEM

The physical modelling of space frame-raft-soil system is represented by the following elements:

(a) Three Noded Parabolic Isoparametric Beam Bending Element with 6 D.O.F per Node

The present beam bending element (Hinton et. al. [10] and Viladkar et. al. [11]) has been used to represent the beams and columns of the superstructure. Moreover the formulation of this element is such that (Noorzaei [12]) it allows for the deformation due to transverse shear (Figure 1 a-c), i. e.,

$$\theta_y = \frac{\partial w}{\partial z} + \phi_z \quad (1)$$

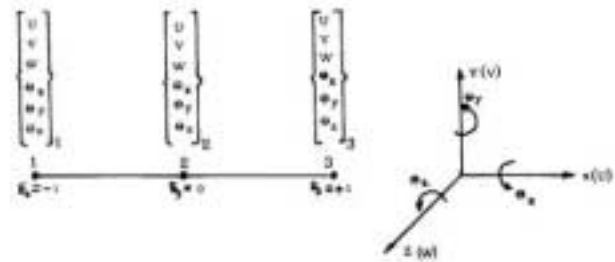
and

$$\theta_z = \frac{\partial v}{\partial x} + \phi_y \quad (2)$$

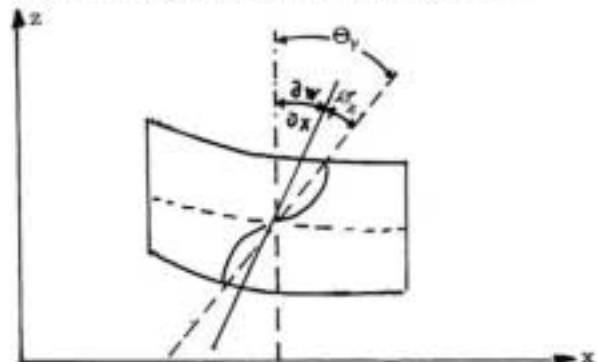
where, ϕ_y and ϕ_z are the rotations due to shear in XZ and XY planes respectively. (Figure 1b-c)

The generalized forces acting on the element section are defined as follows:

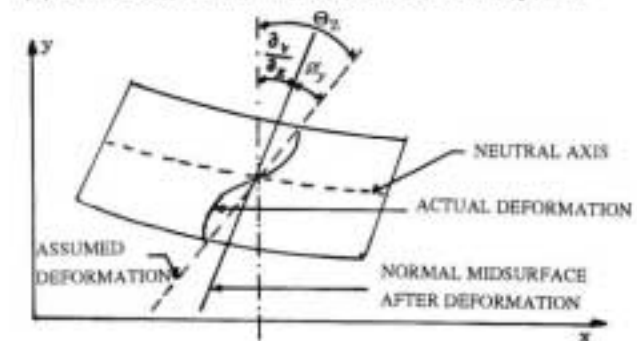
$$\text{Axial forces: } P_x = A E \frac{\partial u}{\partial x} \quad (3)$$



(a) Parabolic Isoparametric Beam Bending Element



(b) Cross-Sectional Deformation of the Beam in x-y Plane



(c) Cross-Sectional Deformation of the Beam in x-z Plane

Figure 1. Three noded isoparametric beam bending element (6 D. O. F/node)

$$\text{Shear forces: } P_y = S \cdot \phi_y = \frac{A G}{\alpha} \left(\theta_z - \frac{\partial v}{\partial x} \right), \text{ and}$$

$$P_z = \frac{A G}{\alpha} \left(\theta_y - \frac{\partial v}{\partial x} \right) \quad (4)$$

$$\text{Bending Moments: } M_y = E I_z \frac{\partial^2 w}{\partial x^2} = E I_z \frac{\partial \theta_y}{\partial x}, \text{ and}$$

$$M_z = E I_y \frac{\partial \theta_x}{\partial x} \quad (5)$$

$$\text{Torsional moment: } M_x = G J \frac{\partial \theta_x}{\partial x} \quad (6)$$

where, A= cross sectional area, $E I_x = E I_y$ = Flexural rigidity, α = Constant which allows for warping effect

= 1.2 (in this case) J = Polar moment of inertia and G = Shear Modulus.

With these pieces of information in hand, the generation of stiffness matrices can be carried out in usual manner.

(b) Eight noded isoparametric plate bending element

This element (Figure 2b) is the modified version of the element presented by Hinton and Owen [10] which includes two additional degrees of freedom due to inplane action. This isoparametric plate bending element can allow for deformation due to transverse shear as:

$$\theta_x = \frac{\partial v}{\partial x} + \phi_x \quad \text{and} \quad \theta_z = \frac{\partial v}{\partial z} + \phi_z \quad (7)$$

where ϕ_x and ϕ_z are the average shear rotation of the midsurface normals as indicated in Figure 2a. The detailed formulation of this element has already been presented by Godbole, et al. [13] and it has been used in this study for the discretization of the structural slab as well as the raft.

(c) Mapped infinite elements

The eight and sixteen noded infinite elements with $1/r$ and $1/\sqrt{r}$ types of decay which are compatible with the eight and sixteen noded isoparametric finite elements have been used for the discretization of the unbounded soil domain. These elements with their functions are presented in Table 1. The coupling of these elements with conventional finite element, their implementation in the finite software, and their validity are explained by Viladkar et al. [14]

TREATMENT OF JUNCTION BETWEEN BEAM, PLATE AND 3-D BRICK ELEMENTS

In the couple finite-infinite elements idealisation of the space frame-raft-soil system, the isoparametric

beam bending element with six D.O.F per node ($u, v, w, \theta_x, \theta_y, \theta_z$) has been used for representing beam and columns, and plate bending element with five D.O.F per node ($u, v, w, \theta_x, \theta_z$) has been used to represent the raft and the structural slabs, while, 3-D brick elements with three D.O.F per node (u, v, w) has been utilised to model the soil media. A typical connection of these three types of elements has been demonstrated in Figure 2 c. The junction between

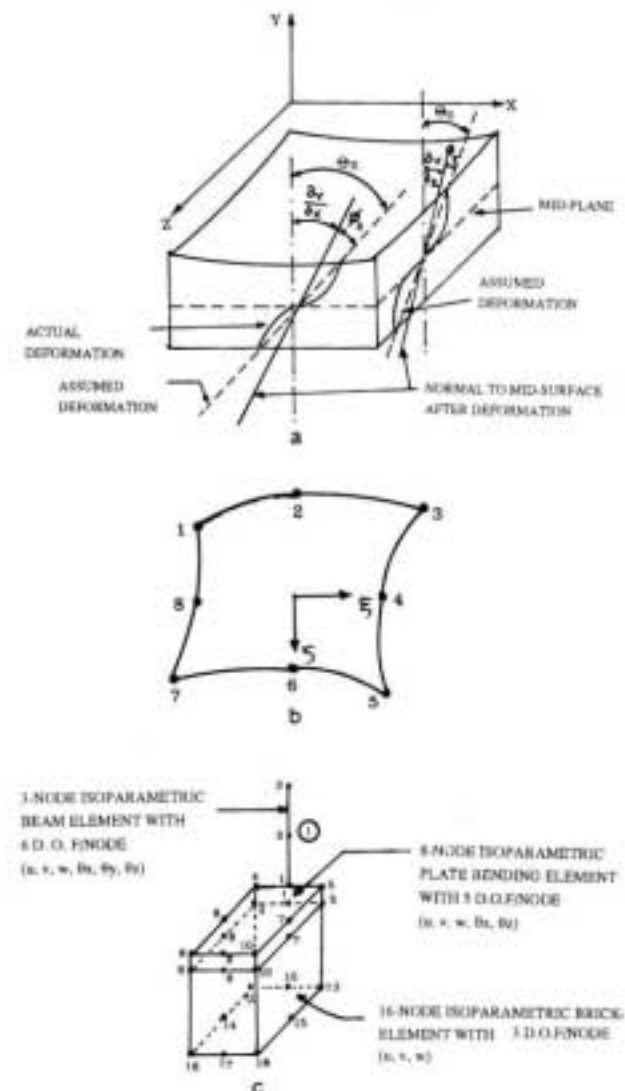
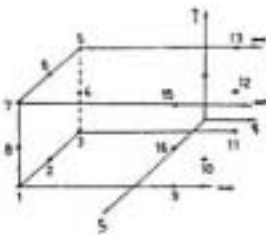


Figure 2(a). Deformation of the cross section of plate of homogeneous section. **(b).** Parabolic isoparametric plate element. **(c).** Junction of beam, plate and brick elements.

Table 1. Mapping/Shape Functions for 3-D Serendipity Type Isoparametric Infinite Elements.

| Type of Element | Element Figure | Mapping/Shape Functions | |
|-----------------|----------------|--|--|
| | | (1/r) type decay | (1/√r) type decay |
| 8 noded | | $N_1 = \frac{-\xi(1-\eta)(1+\zeta)}{2(1-\xi)}$ | $\frac{1}{3} \left[1 - \frac{1}{(1-\xi)^2} \right] (1-\eta)(1+\zeta)$ |
| | | $N_2 = \frac{-\xi(1-\eta)(1-\zeta)}{2(1-\xi)}$ | $\frac{1}{3} \left[1 - \frac{1}{(1-\xi)^2} \right] (1-\eta)(1-\zeta)$ |
| | | $N_3 = \frac{-\xi(1+\eta)(1-\zeta)}{2(1-\xi)}$ | $\frac{1}{3} \left[1 - \frac{1}{(1-\xi)^2} \right] (1+\eta)(1-\zeta)$ |
| | | $N_4 = \frac{-\xi(1+\eta)(1+\zeta)}{2(1-\xi)}$ | $\frac{1}{3} \left[1 - \frac{1}{(1-\xi)^2} \right] (1+\eta)(1+\zeta)$ |
| | | $N_5 = \frac{(1+\xi)(1-\eta)(1+\zeta)}{4(1-\xi)}$ | $\frac{1}{12} \left[\frac{4}{(1-\xi)^2} - 1 \right] (1-\eta)(1+\zeta)$ |
| | | $N_6 = \frac{(1+\xi)(1-\eta)(1-\zeta)}{4(1-\xi)}$ | $\frac{1}{12} \left[\frac{4}{(1-\xi)^2} - 1 \right] (1-\eta)(1-\zeta)$ |
| | | $N_7 = \frac{(1+\xi)(1+\eta)(1-\zeta)}{4(1-\xi)}$ | $\frac{1}{12} \left[\frac{4}{(1-\xi)^2} - 1 \right] (1+\eta)(1-\zeta)$ |
| | | $N_8 = \frac{(1+\xi)(1+\eta)(1+\zeta)}{4(1-\xi)}$ | $\frac{1}{12} \left[\frac{4}{(1-\xi)^2} - 1 \right] (1+\eta)(1+\zeta)$ |
| 12 noded | | $N_1 = \frac{-\xi(1-\eta)(1+\zeta)}{2(1-\xi)}$ | $\frac{1}{3} \left[1 - \frac{1}{(1-\xi)^2} \right] (1-\eta)(1+\zeta)$ |
| | | $N_2 = \frac{-\xi(1-\eta)(1-\zeta^2)}{(1-\xi)}$ | $\frac{2}{3} \left[1 - \frac{1}{(1-\xi)^2} \right] (1-\eta)(1-\zeta^2)$ |
| | | $N_3 = \frac{\xi(1-\eta)\zeta(1-\zeta)}{2(1-\xi)}$ | $-\frac{1}{3} \left[1 - \frac{1}{(1-\xi)^2} \right] (1-\eta)(1-\zeta)$ |
| | | $N_4 = \frac{\xi(1+\eta)\zeta(1-\zeta)}{2(1-\xi)}$ | $-\frac{1}{3} \left[1 - \frac{1}{(1-\xi)^2} \right] (1+\eta)\zeta(1-\zeta)$ |
| | | $N_5 = \frac{-\xi(1+\eta)(1-\zeta^2)}{(1-\xi)}$ | $\frac{2}{3} \left[1 - \frac{1}{(1-\xi)^2} \right] (1+\eta)(1-\zeta^2)$ |

(Table 1. Contd...)

| (1) | (2) | (3) | (4) |
|----------|---|---|---|
| | | $N_6 = \frac{-\xi(1+\eta)\zeta(1+\zeta)}{2(1-\xi)}$ | $\frac{1}{3}\left[1 - \frac{1}{(1-\xi)^2}\right](1+\eta)\zeta(1+\zeta)$ |
| | | $N_7 = \frac{(1+\xi)(1-\eta)\zeta(1+\zeta)}{4(1-\xi)}$ | $\frac{1}{12}\left[\frac{4}{(1-\xi)^2} - 1\right](1-\eta)\zeta(1+\zeta)$ |
| | | $N_8 = \frac{(1+\xi)(1-\eta)(1-\zeta^2)}{2(1-\xi)}$ | $\frac{1}{6}\left[\frac{4}{(1-\xi)^2} - 1\right](1-\eta)(1-\zeta^2)$ |
| | | $N_9 = \frac{-(1+\xi)(1-\eta)\zeta(1-\zeta)}{4(1-\xi)}$ | $-\frac{1}{12}\left[\frac{4}{(1-\xi)^2} - 1\right](1-\eta)\zeta(1-\zeta)$ |
| | | $N_{10} = \frac{-(1+\xi)(1+\eta)\zeta(1-\zeta)}{4(1-\xi)}$ | $-\frac{1}{12}\left[\frac{4}{(1-\xi)^2} - 1\right](1+\eta)\zeta(1-\zeta)$ |
| | | $N_{11} = \frac{(1+\xi)(1+\eta)(1-\zeta^2)}{2(1-\xi)}$ | $\frac{1}{6}\left[\frac{4}{(1-\xi)^2} - 1\right](1+\eta)(1-\zeta^2)$ |
| | | $N_{12} = \frac{(1+\xi)(1+\eta)\zeta(1+\zeta)}{4(1-\xi)}$ | $\frac{1}{12}\left[\frac{4}{(1-\xi)^2} - 1\right](1+\eta)\zeta(1+\zeta)$ |
| 16 noded |  | $N_1 = \frac{-\xi(1-\eta)(\zeta-\eta-1)(1+\zeta)}{2(1-\xi)}$ | $\frac{1}{3}\left[1 - \frac{1}{(1-\xi)^2}\right](1-\eta)(\zeta-\eta-1)(1+\zeta)$ |
| | | $N_2 = \frac{-\xi(1-\eta)(1-\zeta^2)}{(1-\xi)}$ | $\frac{2}{3}\left[1 - \frac{1}{(1-\xi)^2}\right](1-\eta)(1-\zeta^2)$ |
| | | $N_3 = \frac{-\xi(1-\eta)(-\zeta-\eta-1)(1-\zeta)}{2(1-\xi)}$ | $\frac{1}{3}\left[1 - \frac{1}{(1-\xi)^2}\right](1-\eta)(-\zeta-\eta-1)(1-\zeta)$ |
| | | $N_4 = \frac{-\xi(1-\eta^3)(1-\zeta)}{(1-\xi)}$ | $\frac{2}{3}\left[1 - \frac{1}{(1-\xi)^2}\right](1-\eta^3)(1-\zeta)$ |
| | | $N_5 = \frac{-\xi(1+\eta)(-\zeta+\eta-1)(1-\zeta)}{2(1-\xi)}$ | $\frac{1}{3}\left[1 - \frac{1}{(1-\xi)^2}\right](1+\eta)(-\zeta+\eta-1)(1-\zeta)$ |
| | | $N_6 = \frac{-\xi(1+\eta)(1-\zeta^2)}{(1-\xi)}$ | $\frac{2}{3}\left[1 - \frac{1}{(1-\xi)^2}\right](1+\eta)(1-\zeta^2)$ |
| | | $N_7 = \frac{-\xi(1+\eta)(\zeta+\eta-1)(1+\zeta)}{2(1-\xi)}$ | $\frac{1}{3}\left[1 - \frac{1}{(1-\xi)^2}\right](1+\eta)(\zeta+\eta-1)(1+\zeta)$ |

(Table 1. Contd...)

| (1) | (2) | (3) | (4) |
|-----|-----|---|---|
| | | $N_8 = \frac{-\xi(1-\eta^2)(1+\zeta)}{(1-\xi)}$ | $\frac{2}{3} [1 - \frac{4}{(1-\xi)^2}] (1-\eta^2)(1+\zeta)$ |
| | | $N_9 = \frac{(1+\xi)(1-\eta)(\zeta-\eta-1)(1+\zeta)}{4(1-\xi)}$ | $\frac{1}{12} [\frac{4}{(1-\xi)^2} - 1] (1-\eta)(-\eta-\zeta-1)(1+\zeta)$ |
| | | $N_{10} = \frac{(1+\xi)(1-\eta)(1-\zeta^2)}{2(1-\xi)}$ | $\frac{1}{6} [\frac{4}{(1-\xi)^2} - 1] (1-\eta)(1-\zeta^2)$ |
| | | $N_{11} = \frac{(1+\xi)(1-\eta)(-\zeta-\eta-1)(1-\zeta)}{4(1-\xi)}$ | $\frac{1}{12} [\frac{4}{(1-\xi)^2} - 1] (1-\eta)(-\eta-\zeta-1)(1-\zeta)$ |
| | | $N_{12} = \frac{(1+\xi)(1-\eta^3)(1-\zeta)}{2(1-\xi)}$ | $\frac{1}{6} [\frac{4}{(1-\xi)^2} - 1] (1-\eta^3)(1-\zeta)$ |
| | | $N_{13} = \frac{(1+\xi)(1+\eta)(-\zeta+\eta-1)(1-\zeta)}{4(1-\xi)}$ | $\frac{1}{12} [\frac{4}{(1-\xi)^2} - 1] (1+\eta)(\eta-\zeta-1)(1-\zeta)$ |
| | | $N_{14} = \frac{(1+\xi)(1+\eta)(1-\zeta^2)}{2(1-\xi)}$ | $\frac{1}{6} [\frac{4}{(1-\xi)^2} - 1] (1+\eta)(1-\zeta^2)$ |
| | | $N_{15} = \frac{(1+\xi)(1+\eta)(\zeta+\eta-1)(1+\zeta)}{4(1-\xi)}$ | $\frac{1}{12} [\frac{4}{(1-\xi)^2} - 1] (1+\eta)(\eta+\zeta-1)(1+\zeta)$ |
| | | $N_{16} = \frac{(1+\xi)(1-\eta^2)(1+\zeta)}{2(1-\xi)}$ | $\frac{1}{6} [\frac{4}{(1-\xi)^2} - 1] (1-\eta^2)(1+\zeta)$ |

these element has been given special treatment by rearranging the global stiffness matrix of beam element for compatibility with the corresponding D. O. F of the plate element. The additional D. O. F of the beam element as well as of plate element are eliminated in the solution procedure by specially developed frontal solver (Godbole et al. [15])

CONSTITUTIVE MODELLING OF SOILS

The stress-strain behavior of soil mass is essentially

nonlinear. The nonlinearity significantly influences the behavior of any structure-foundation-soil system. In most of the early investigations into soil-structure interaction phenomenon, it is assumed that the stress-strain response of the soil mass is linear, particularly because the solution is then achieved in a single step. In this study, an attempt is made to account for actual nonlinear behavior of soil obtained from triaxial test data.

Due to the generality of the hyperbolic model and its ability to represent the stress-strain behavior of

soil ranging from clays and silts through sands, gravels and rockfills, it can be used for partly or fully saturated soils, and for drained or undrained loading conditions in compacted earth materials or naturally occurring soils (Duncan, [16]). Hence it is possible to make use of such a model in the nonlinear interactive analysis of framed structure-foundation soil interaction for predicting the behavior of the structure. Moreover, its implementation in the finite element software is not complex.

On the basis of the hyperbolic approach suggested by Kondner, et al. [17] and Duncan, et.al. [18], the tangent Young's modulus and tangent Poisson's ratio of soil are expressed as

$$E_T = \left[1 - \frac{R_f (1 - \sin \phi) (\sigma_1 - \sigma_3)^2}{2(c \cos \phi + \sigma_3 \sin \phi)} \right]^2 E_i \quad (8)$$

and

$$\nu_T = \frac{G - F \text{Log} \left(\frac{\sigma_1}{P_a} \right)}{\left[1 - \frac{(\sigma_1 - \sigma_3)d}{A} \right]^2} \quad (9)$$

where,

$$E_i = K P_a \left(\frac{\sigma_3}{P_a} \right)^n \quad (10a)$$

and

$$A = \left[1 - \frac{R_f (1 - \sin \phi) (\sigma_1 - \sigma_3)}{2(c \cos \phi + \sigma_3 \sin \phi)} \right] E_i \quad (10b)$$

$$R_f = (\sigma_1 - \sigma_3)_{it} / (\sigma_1 - \sigma_3)_{ult} \quad (10c)$$

where,

c = cohesion,

R_f = failure ratio,

ϕ = Angle of internal friction

k = modulus number

P_a = atmospheric pressure

n = exponent

G = the value of ν_i at unit atmospheric pressure

F = the rate of change of initial poisson ratio, ν_i with confining pressure, σ_3

d = the parameter expressing rate of change of ν_i with strain

However, in this study a constant value of poisson's ratio, is chosen and the tangent modulus E_T has been varied in the analysis on the basis of the stress level.

NUMERICAL EXAMPLE

Definition of the problem

The proposed physical model has been used for the interactive analysis of a four storey, five bay by three bay space frame-raft soil system (King et al. [3,4,5]).

Figure 3a shows the isometric view of the space frame raft-soil system. The layout details of the frame are shown in Figure 3b. Figures 3c and 3d show the front and side elevations of the frame along with other details. The geometrical details of the frame, its components and the raft are presented in Table 2. Figure 4 shows the coupled finite-infinite element discretization of the entire system including superstructure, raft and soil medium using a quarter

Table 2. Geometrical details of space frame and raft

| Sl. No. | Structure | Component | Size |
|---------|-----------------|--|-------------|
| (1) | (2) | (3) | (4) |
| 1. | Frame | No. of storeys | 4 |
| | | No. of bays | 5×3 |
| | | Storey height (m) | 3.5 |
| | | Bay width (m) | 5.0 |
| | | All beams (m×m) | (0.30×0.61) |
| | | Interior columns of ground and first floor (m×m) | (0.40×0.40) |
| | | Other columns (m×m) | (0.36×0.36) |
| 2. | Raft | Plan size (m×m) | (25.×15.) |
| | | Thickness (m) | 0.40 |
| 3. | Structural slab | Thickness (m) | 0.15 |

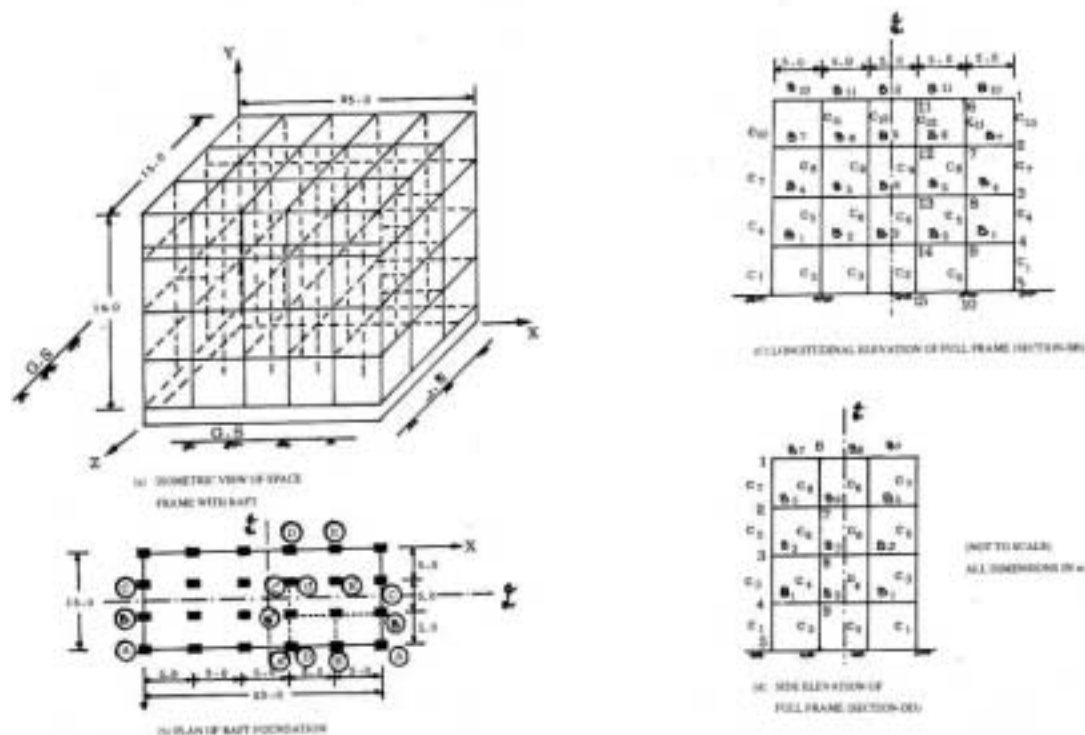


Figure 3. Geometric details of the space frame

symmetry. Figure 4 also shows the discretization of top floor slab in detail. The slabs of other floors have also been idealized in a similar manner. The loading pattern on the structure and the raft are shown in the Figure 5.

The validity of the proposed physical model and the behavior of the space frame with and without slab effect have been already discussed in detail by Godbole, et al. [13] Here, the effect of soil nonlinearity has been highlighted and the entire nonlinear analysis has been carried out by using the iterative solution technique.

SOIL NONLINEARITY

In order to consider the effect of soil nonlinearity, normally the stress-strain curve for soil obtained from laboratory triaxial tests, for different confining pressures should be considered. In the present study, the range of the nonlinear soil parameters presented by Duncan [16] is considered. Table 3 shows the

numerical values of various soil parameters such as, k , n , R_f etc. (Equations 10a, b, and c) required to determine the tangent modulus of soil, E_T , (Equation 8) at any deviatoric stress level in soil. The initial tangent modulus of soil, E_i has been considered to

Table 3. Soil constants required to define hyperbolic model (Duncan [16])

| Sl. No. | Constants | Symbol | Value |
|---------|---|--------|--------|
| (1) | (2) | (3) | (4) |
| 1. | Angle of shearing resistance in degrees | ϕ | 3.0° |
| 2. | Intercept of transformed hyperbola | K | 150.00 |
| 3. | Cohesion (kn/m ²) | c | 50.0 |
| 4. | Slope of transformed hyperbola | n | 0.00 |
| 5. | Failure ratio | R_f | 0.85 |

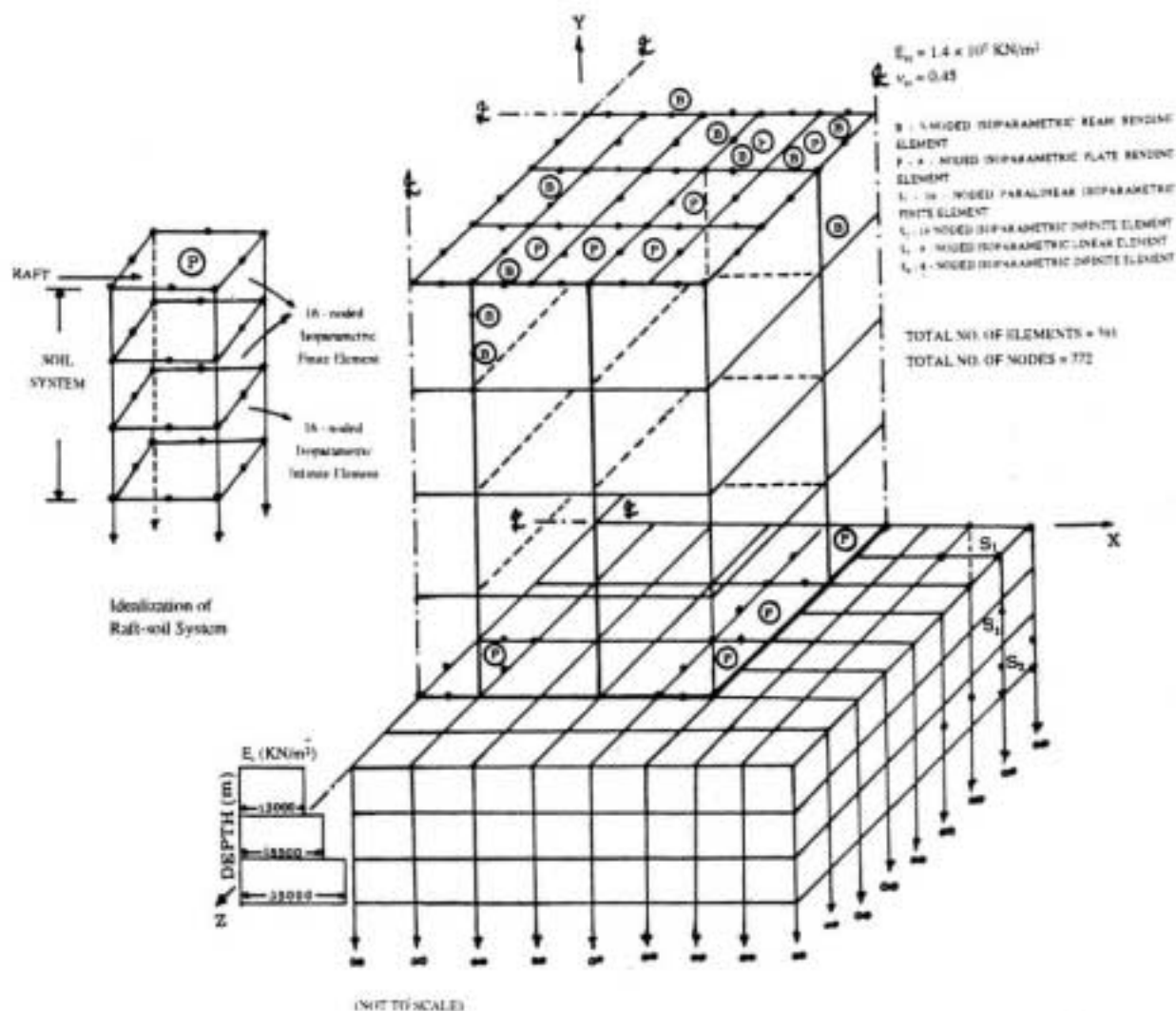


Figure 4. Multielement idealisation of structure-raft-soil system including structural slabs

vary with depth in order to account for soil nonhomogeneity of which the variation is presented in the Figure 4.

Raft Settlements

The total settlement, the differential settlement, and the angular distortion of the raft, defined as a ratio of differential settlement to the spacing between the center and corner of the raft, have been presented in the Table 4 for the sake of comparison for both the linear and nonlinear analyses. It has been observed that for the frame under study, although the total settlement of the raft obtained by the nonlinear

analysis is on higher side as compared to that of linear analysis, the difference in the differential settlement, which is a major factor in altering the behavior of the superstructure, is marginal. The deformation profiles of the raft in the longitudinal direction along sections AA', BB', and CC', (Figure 3b), are presented in Figure 6 for both analyses. Similar plots in the transverse direction for the raft are shown in Figure 7 for sections A'B'C, DD' and CC' and EE' (Figure 3b). It has been found that the nonlinear interactive analysis yields 1.5 to 2 times higher values of settlements than those due the linear interactive analysis.

Table 4. Comparison of total and differential settlements and angular distortion of raft

| Type of interactive analysis | Corner of the raft (mm) | Centre of the raft (mm) | Differential settlement (mm) | Angular Distortion between centre and corner of raft $\times 10^{-3}$ rad |
|------------------------------|----------------------------|----------------------------|---------------------------------|--|
| (1) | (2) | (3) | (4) | (5) |
| Linear | 17.32 | 27.20 | 9.88 | 0.677 |
| Nonlinear | 27.29 | 39.10 | 11.81 | 0.810 |

Contact Pressure

The contact pressure distribution below the raft has been plotted in Figure 8 for the longitudinal direction along sections A A', BB' and CC' and in Figure 9 for the transverse direction along sections A'B'C', DD' and EE'. The contact pressure is made non-dimensional with respect to total pressure intensity, q (=total load/Area of raft=6.2 t/m²). It is obvious from these plots that the material non-linearity of the soil plays a major role in redistribution of the stresses

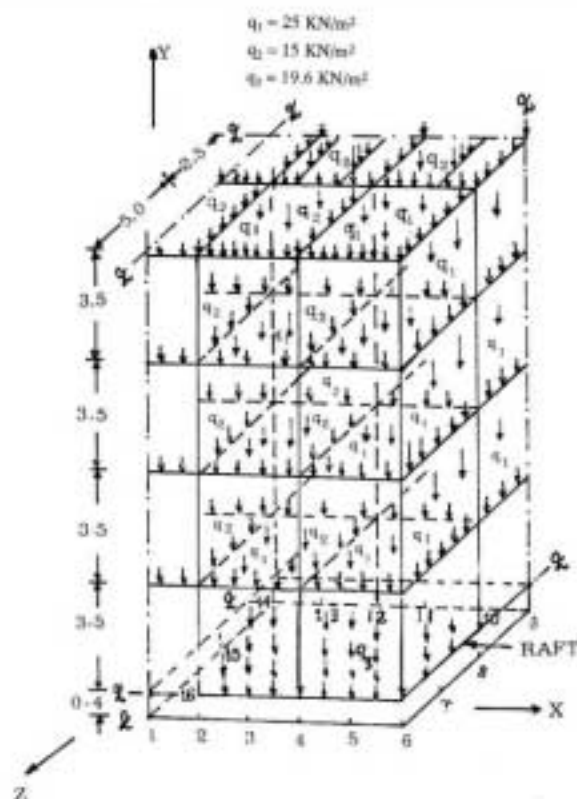


Figure 5. Settlement profile of the raft in longitudinal direction

in the sub-soil, which is intune with the calculation of the unbalance force = $\left[\int B^T \sigma dv - \{R\} \right]$. Moreover the scattered variation in contact pressure via nonlinearity for the sections-BB and A B C is logical as the total applied (soil reaction) must be equal to the total

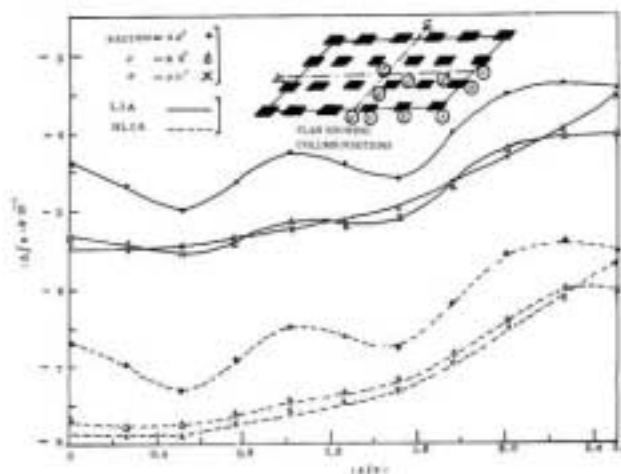


Figure 6. Settlement idealisation of structure - raft - soil system including structural slabs

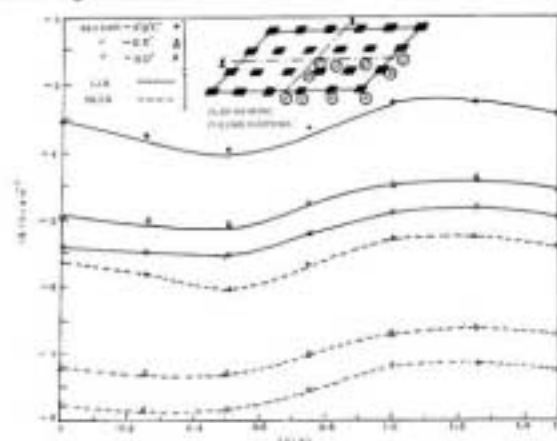


Figure 7. Settlement profile of the raft in transverse direction

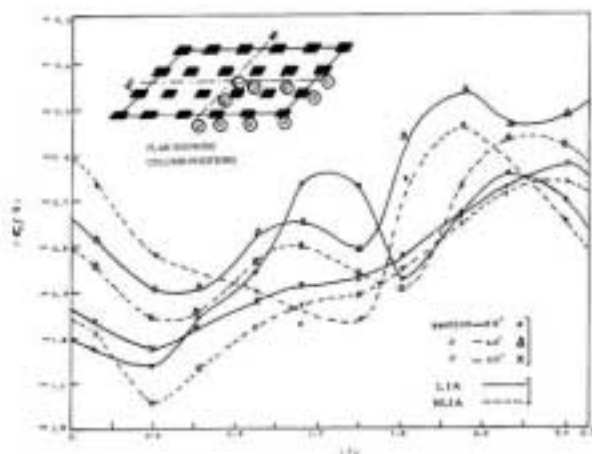


Figure 8. Contact pressure distribution below the raft in longitudinal direction

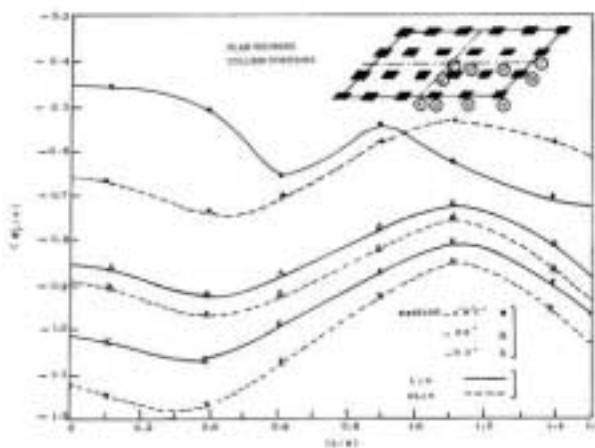


Figure 9. Contact pressure distribution below the raft in transverse direction

externally applied load on the structure foundation system.

Bending Moments

(a) Raft

Figures 10 and 11 show, respectively, the variation of the bending moments M_x , and M_z in the longitudinal direction along sections AA', BB' and CC'. It has been noticed that the soil nonlinearity has just marginal effect on the bending moment variation in the raft at these sections. It can be said that the bending moments in the raft will be influenced mainly due to the magnitude of the differential settlement and relative stiffness between raft and soil media.

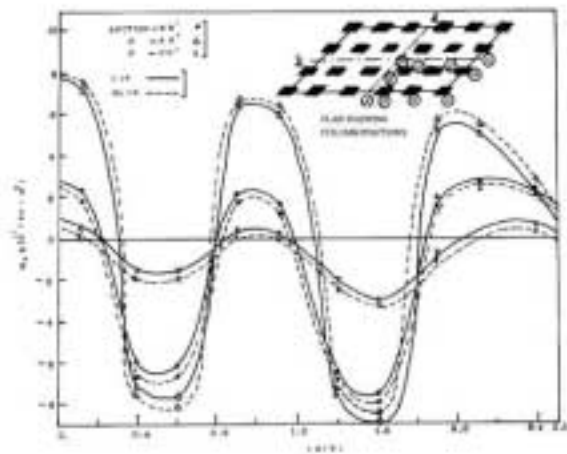


Figure 10. Variation of moment M_x in the raft in longitudinal direction

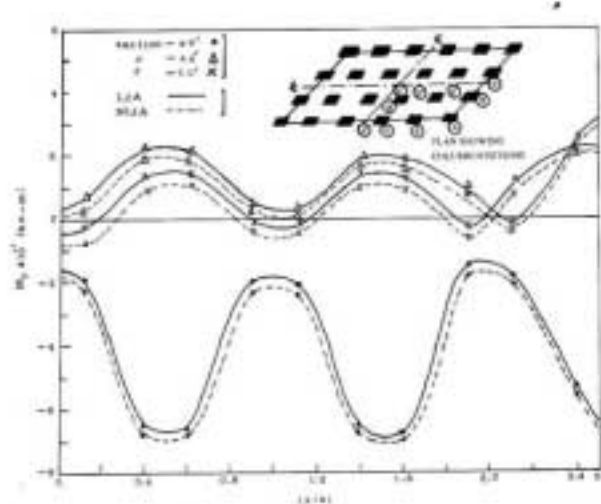


Figure 11. Variation of moment M_z in the raft in longitudinal direction

(b) Frame

i) Moments

The comparison of bending moment, M_x in the longitudinal direction along section-BB' is presented in Table 5 for the beams and columns of first, third and fourth storey levels (columns-4 and 5) for linear and nonlinear interactive analyses. Column-6 shows the departure in the values of moments due to soil nonlinearity, which is in the range of -22 to +9 percent. On the basis of the detail study of results (not included here due to limitation of the space), it has been found that the bending moment, M_x obtained via

Table 5. Bending moment, M (kg-m) variation for linear and nonlinear interactive analyses in longitudinal direction (section-BB')

| Floor | Member | Ends | LIA | NLIA | % difference bent. 4 & 5 |
|----------------|-----------------|-----------------|----------|----------|--------------------------|
| (1) | (2) | (3) | (4) | (5) | (6) |
| I | B ₁ | 4 | -4179.80 | -4592.29 | +9.82 |
| | | 9 | 1980.40 | 1541.90 | -22.14 |
| | B ₂ | 9 | -3819.37 | -4049.69 | +6.00 |
| | | 14 | 2950.90 | 2722.19 | -7.75 |
| | B ₃ | 14 | -3486.50 | -3491.19 | +0.13 |
| | III | B ₇ | 2 | -5271.70 | -5580.76 |
| 7 | | | 1503.00 | 1190.00 | -20.80 |
| B ₈ | | 10 | -3750.00 | -3887.59 | +3.67 |
| | | 12 | 2839.53 | 2670.00 | -5.97 |
| B ₉ | | 12 | -3332.93 | -3315.54 | -0.52 |
| IV | | B ₁₀ | 1 | -3420.80 | -3612.00 |
| | 6 | | 2381.16 | 2178.56 | -8.50 |
| | B ₁₁ | 6 | -3539.38 | -3596.67 | +1.60 |
| | | 11 | 2974.60 | 2855.27 | -4.00 |
| | B ₁₂ | 11 | -3270.16 | -3237.00 | -1.00 |
| | I | C ₁ | 5 | 638.87 | 1349.93 |
| 4 | | | 2250.10 | 3102.55 | +21.67 |
| C ₂ | | 10 | 1792.37 | 2601.00 | +45.20 |
| | | 9 | 908.00 | 1603.00 | +76.54 |
| C ₃ | | 15 | 274.00 | 592.99 | ** |
| | | 14 | 414.89 | 662.33 | +59.96 |
| IV | C ₁₀ | 2 | 5455.28 | 5738.77 | +5.20 |
| | | 1 | 6685.34 | 7025.63 | +5.10 |
| | C ₁₁ | 7 | 1690.51 | 2058.30 | +21.74 |
| | | 6 | 1723.51 | 2129.15 | +23.45 |
| | C ₁₂ | 12 | 393.28 | 576.70 | +31.38 |
| | | 11 | 459.21 | 359.70 | +21.67 |

** Correspond to Percentage difference above 100 percent.

nonlinear analysis is, in general, on the higher side. In particular, the nature of moment, M_x in the column members at the first storey level has changed due to soil nonlinearity. The variation in the column moments is of the order 20 to 75 percent. This fact can be due to redistribution of the contact pressure in soil mass below the raft. Similar behavior is also reported by King et al. [6].

ii) Axial Forces in Columns

The values of the axial forces in the column members at various storey levels at section-BB' for both the linear and nonlinear interactive analyses are presented in Table 6. A glance at this table evinces that axial forces have been reduced just marginally by about 2 percent at this particular section due to soil nonlinearity.

Convergence

In order to illustrate the nature of convergence achieved during the solution procedure, variation, i. e., reduction in the norm of the residual forces with respect to the iterations is plotted in Figure 12. It is clear that a convergence with the reduction of the residual force to just 2 percent was achieved in just 9 iterations.

CONCLUSIONS

i) The proposed physical model of the space

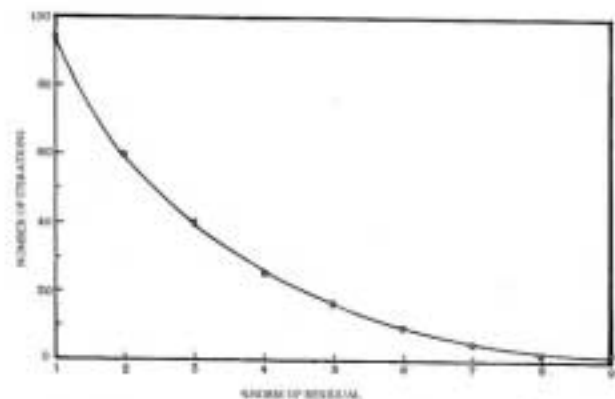


Figure 12. Variation of norm of force-residual with number of iteration

Table 6. Axial forces (kn) in the columns at various storey levels (Section-BB')

| Storey level | Members | LIA | NLIA |
|--------------|-----------------|--------|--------|
| (1) | (2) | (3) | (4) |
| IV | C ₁₂ | 202.58 | 199.30 |
| | C ₁₁ | 204.87 | 200.00 |
| | C ₁₀ | 112.05 | 110.00 |
| III | C ₉ | 403.20 | 395.90 |
| | C ₈ | 403.80 | 396.00 |
| | C ₇ | 233.24 | 230.40 |
| II | C ₆ | 603.50 | 591.90 |
| | C ₅ | 609.99 | 597.60 |
| | C ₄ | 351.10 | 346.70 |
| I | C ₃ | 806.30 | 789.40 |
| | C ₂ | 815.20 | 797.60 |
| | C ₁ | 471.00 | 465.00 |

frame-raft-soil system is an improved form of physical modelling of the system.

ii) The finite element discretization which includes the slab as part of the superstructure is the most natural way of the representation of the space frame-raft-soil mass system.

iii) Based on the type of the problem studied in this investigation, the non-linear interactive analysis using the hyperbolic constitutive models produces the following:

(a) Differential settlements have increased,

(b) Further redistribution of the contact pressures beneath the raft is achieved.

(c) Nominal effect in the values of moment, M_x in beams at section-BB' is observed, while the section-AA' has experienced further redistribution in the M_x values.

(d) The column moments at these two sections have substantially increased by about 76 percent.

(e) The axial forces in the column members have reduced only nominally (Section-BB').

iv) The iterative solution technique is best suited

for such a three dimensional type of the problems and results in substantial saving in the computational time and effort.

REFERENCES

1. M. J. Haddadian, "Mats and Combined Footing by the Finite Element Method". *ACI*, Vol. 68, No. 12, (1971) pp. 945-949.
2. S. J. Hain and I. K. Lee, "Rational Analysis of Raft Foundation", *Jnl. Geotech. Engg. Div., ASCE*, No. 3, (1974) pp. 481-488.
3. G. J. W. King and V. S. Chandrasekaran, "Interactive Analysis of Rafted Multi-storeyed Space Frame Resting in an Inhomogeneous Clay Stratum", Proc. Int. Conf. on F. E. M. in Engg., Univ. of New South Wales, Australia, pp. (1974) 493-509.
4. G. J. W. King, "An Introduction to Superstructure/Raft/soil Interaction", Proc. Int. Symp. on soil-structure interaction, University of Roorkee, India, Vol. 1, (1977) pp. 453-466.
5. King and Z. E. Yao, "Simplified Interactive Analysis of Long Framed Building on Raft Foundation", *Jnl. Struct. Engineer*, Vol. 61, (B-3), (1983) pp. 62-67.
6. K. S. Sankaran and R. Srinivasaraghavan, "Soil-Structure-Interaction-A Parametric Study", Proc. Int. Conf. on Computer Application in Civil Engg., U. O. R., Roorkee, India, Theme-VII, (1979) pp. 7-12.
7. R. Srinivasaraghavan and K. S. Sankaran, "Settlement Analysis for Combined Effect of Superstructure-Footings-Soil System", *Jnl. of Engrs. (India)*, Vo. 63, Part C14, (1983) PP. 194-198.
8. G. C. Nayak, S. K. Agarwal and S. C. Chakrabarti, "Effect of Sequence of Construction in 2D and 3D multistoreyed Building" Proc. Int. Conf. on Computer Application in Civil Engg., Univ. of Roorkee, India, Theme-VII, (1985) pp. 7-12.
9. P. T. Brown and K. R. Yu, "Load Sequence and Soil-Foundation-Interaction", *Jnl. of Struct., Div., ASCE*, Vol. 112, No. 3, (1966) pp. 481-488.
10. E. Hinton and D. R. J. Owen, "Finite Element

Programming", Academic Press, London (1977).

11. M. N. Viladkar, P. N. Godbole and J. Noorzai, "Soil-Structure Interaction in plane Frames using Coupled Finite-Infinite Elements", *Int. Jnl. Comput. and Struct.* Vol. 39, No. 5, (1991).
12. J. Noorzai, "Non-linear Soil Structure Interaction in Framed Structure", Ph. D. thesis, in Civil Engg. Deptt., University of Roorkee, India (1991).
13. P. N. Godbole, M. N. Viladkar and J. Noorzai, "Space Frame-Raft soil Interaction including Effect of Slab Stiffness", *Int. Jnl. of Comput. Struct.*, Vol. 43, No.1, (1992) pp. 93-106.
14. M. N. Viladkar, P. N. Godbole and J. Noorzai, "Some New Three Dimensional Infinite Elements", *Int. Jnl. Comput. and Struct.* Vol. 34, No. 3, (1990) pp. 455-467.
15. P. N. Godbole, M. N., Viladkar and J. Noorzai, "A Modified Frontal Solver with Multi-element and variable degrees of Freedom Features", *Int. Jnl. of Computer and Structures*, Vol. 39, No. 5, (1991) pp. 525-534.
16. J. M. Duncan, "Hyperbolic Stress-Strain Relationships", ASCE, Proc. of the Workshop on Limit Equilibrium, Plasticity and Generalized Stress-Strain in Geotech. Engg., Mc-Gill Univ., Montreal, Canada, (1980) pp. 443-460.
17. R. L. Konder and J. B. Zelasko, "A Hyperbolic Stress-Strain Formulation of Sands", Proc. 2nd Pan-American, Conf. On SMFE, Brazil, Vo; 1, (1963) pp. 289-324.
18. J. M. Duncan and C. Y. Chang, "Nonlinear Analysis of Stress and Strain in Soils", *Jnl. SMFE, ASCE, Div.*, Vol. 96, No. 5, (1970) pp. 1629-1653.